A Platinum Open Access Journal for Organic Chemistry

Paper

Free to Authors and Readers

DOAJ Seal

Arkivoc **2023**, part iii, 0-0
to be inserted by editorial office

Highly chemoselective conjugate addition of lithium tetraorganozincates to coumarin derivatives and functionalization with electrophiles

Marzia Dell'Aera,[a,b] Filippo Maria Perna,[b] Paola Vitale,[b] Antonio Salomone,[c] Angela Altomare,[a] and Vito Capriati*[b]

[a] *Istituto di Cristallografia (IC-CNR), Via G. Amendola 122/o, 70125 Bari, Italy*
[b] *Dipartimento di Farmacia-Scienze del Farmaco, Università degli Studi di Bari "Aldo Moro", Consorzio C.I.N.M.P.I.S., Via E. Orabona 4, 70125, Bari, Italy*
[c] *Dipartimento di Chimica, Università degli Studi di Bari "Aldo Moro", Consorzio C.I.N.M.P.I.S., Via E. Orabona 4, 70125, Bari, Italy*
Email: vito.capriati@uniba.it

Dedicated to Professor Saverio Florio for his contribution to synthetic organic chemistry

Received mm-dd-yyyy **Accepted Manuscript** mm-dd-yyyy **Published on line** mm-dd-yyyy

Dates to be inserted by editorial office

Abstract

The nucleophilic addition (alkylation/arylation) of lithium tetraorganozincate species (R_4ZnLi_2) to coumarin derivatives takes place cleanly, with a short reaction time (30 min) and with high chemoselectivity, when working under mild conditions (0 °C) and with no additional solvents. Particularly remarkable is the diastereoselectivity of the reaction (up to 96:4), after trapping the resulting intermediates with external electrophiles. The stereochemistry of the major trisubstituted stereoisomer was assigned by combining 2D NOESY experiments with DFT calculations.

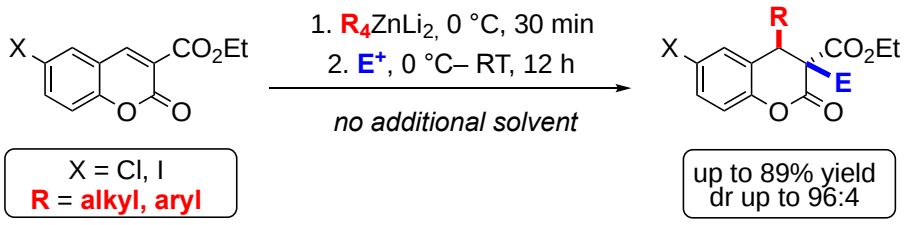

Keywords: Coumarin derivatives, nucleophilic additions, zincate species, external trapping

Introduction

Recently, alkali-metalated species have received considerable attention in the synthetic organic chemistry field.[1,2] For instance, lithium nickelates proved to be key intermediates in Ni-catalyzed cross-coupling reactions of aryl ethers in the co-complexation chemistry of PhLi with $Ni(COD)_2$.[3] Higher-order homoleptic lithium manganates have also been found to promote direct Mn-I exchange reactions of aryl iodides,[4] whereas sodium and potassium magnesiates have revealed to act as powerful catalysts in promoting hydroamination processes at room temperature[5] or as effective pre-catalysts for the synthesis of novel 1,5-disubstituted triazoles.[6] On our side, we have recently reported on the first transition metal catalyst- and ligand-free conjugate addition of lithium tetraorganozincates to nitroolefins *en route* to valuable nitroalkanes in up to 98% yield, while working under mild conditions (0 °C) and a short reaction time (30 min).[7] In light of such results, we wondered whether the enhanced nucleophilicity and the unique chemoselectivity displayed by these higher-order zincates could be extended to other kind of nucleophilic addition reactions, such as those towards α,β-unsaturated carbonyl compounds that are an important class of C–C bond-forming reactions in organic chemistry.[8,9]

Coumarin derivatives are essential heterocyclic scaffolds in medicinal chemistry as they display a broad array of pharmacological and biological properties as anticancer,[10] antibacterial,[11] anticoagulant,[12] against Alzheimer's disease,[13] and are also widely used as fluorescent probes and chemosensors in the treatment of neurodegenerative diseases,[14] and as light absorbers for solar cells and organic light emitting diodes.[15,16] Ethyl coumarin-3-carboxylate (**1**) is, in particular, a key player in organic synthesis for the preparation of biologically active compounds.[17] Thus, selective functionalization of this skeleton is highly sought after. The organometallic-mediated conjugate addition to the unsaturated lactone ring of **1**, however, is known to proceed with poor chemoselectivity and yield. In 1975, Gustafsson reported that the reaction of **1** with *t*-BuMgCl led to a mixture of products including adduct **3** (as the result of the attack on the ester group) and the homodimerized product **4**, beyond adduct **2** [Scheme 1A, Eq. (1)].[18] Two years later, Gustafsson and Ostman described the reaction of *o*-tolylmagnesium bromide with **1** to give adduct **5** in 25% yield only, after 48 h reaction time [Scheme 1B, Eq. (2)].[19] A Noyori-type organocopper reagent, namely lithium (*Z*)-2-ethoxyethenylbis(tributylphosphine)cuprate, preparated in situ by *cis*-1-bromo-2-ethoxyethene, *t*-BuLi, CuI and Bu_3P, was found to promote a conjugate addition to **1** in Et_2O at –78 °C to give adduct **6** in 89% yield [Scheme 1C, Eq. (3)].[20]

Herein, we report that the conjugate addition to coumarins **7a**,**b**, followed by trapping reactions with external electrophiles, can be cleanly carried out when working with high-order zincate species. We showcase that these reactions proceed *i*) with high chemo- and diastereoselectivity (up to 96:4), *ii*) under mild conditions (0 °C) and a short reaction time (30 min), and *iii*) with the desired adducts (±)-**8** isolated in up to 89% yield [Scheme 1D, Eq. (4)].

Previous work:

*A. Conjugate Addition of t-BuMgCl to ethyl coumarin-3-carboxylate (**1**) (ref. 18)*

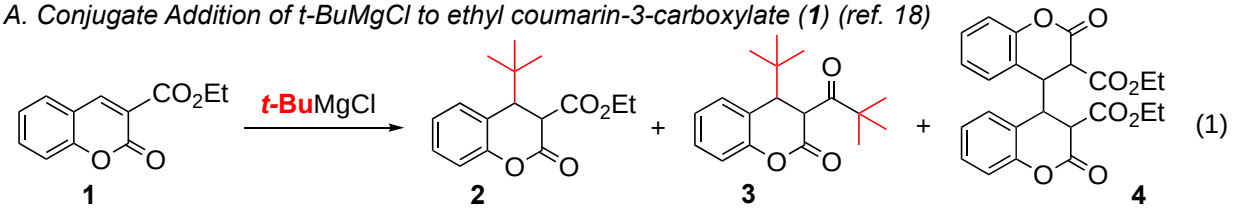

*B. Conjugate addition of 2-tolylMgBr to ethyl coumarin-3-carboxylate (**1**) (ref. 19)*

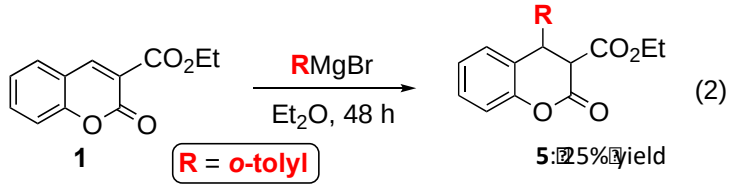

*C. Conjugate addition of (Z)-2-ethoxyvinyl anion to ethyl coumarin-3-carboxylate (**1**) (ref. 20)*

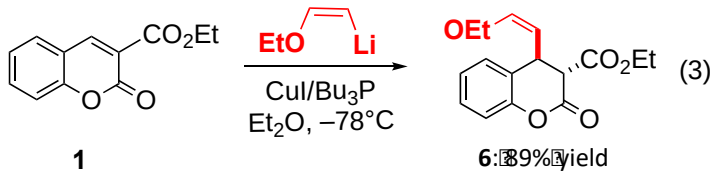

This work:

*D. Conjugate addition of alkali-metal zincate species to coumarins **7a**,**b** and subsequent trapping with an external electrophile to give educts **8***

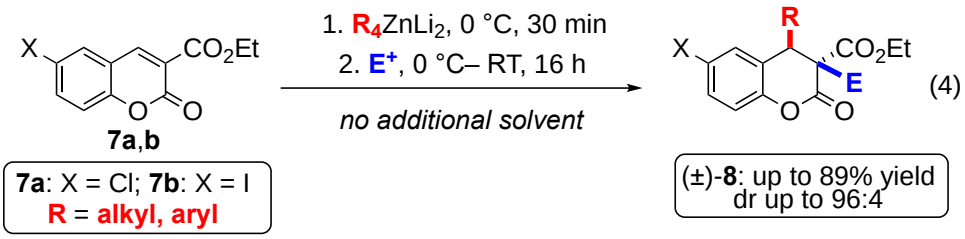

Scheme 1. Conjugate addition of *t*-BuMgCl to ethyl coumarin-3-carboxylate (**1**) (A); conjugate addition of *o*-tolylMgBr to **1** (B); conjugate addition of (*Z*)-2-ethoxyvinyl anion to **1** (C); conjugate addition of high-order zincate species to coumarins **7a**,**b** and subsequent trapping with an external electrophile, to give adducts (±)-**8** (D). RT= room temperature; dr = diastereomeric ratio.

Results and Discussion

We started our investigation using coumarin **7a** as the model substrate, which is amenable to be further functionalized in its backbone through the halogen atom at the 6-position. As can be seen from the results compiled in Table 1, when **7a** was reacted with EtLi (0 °C, 30 min), followed by the addition of BnBr, a complex mixture of products was obtained, which was not further analyzed. On the other hand, by replacing EtLi with Et_2Zn, no reaction took place. Conversely, switching monometallic compounds for homoleptic alkali-metal zincate complexes like Et_3ZnLi and Et_4ZnLi_2 as carbon nucleophiles, the conjugated addition/trapping reaction occurred smoothly, at 0 °C under inert conditions and with no additional solvents, thereby furnishing the desired adduct (±)-**8a** both in remarkable yield (71–89%) and diastereoselectivity [up to 90:10, in favor of the

(3*R**,4*R**)-diastereomer] (*vide infra*) (Table 1, entries 1–4). It is important to highlight the high chemoselectivity of the studied process, as we do not observe *i*) any metal-halogen exchange reaction; or *ii*) competitive nucleophilic addition to the ester group. To the best of our knowledge, the only example of conjugate addition-electrophile trapping of coumarins has so far been reported by Feringa. It refers to a Cu-catalyzed asymmetric conjugate addition of Grignard reagents to coumarins under cryogenic conditions (up to –72 °C) in *t*-butyl methyl ether as the solvent, and in the presence of a reversed Josiphos ligand. The enolate of conjugate addition was trapped with PhCHO (5 equiv), furnishing a *trans*-disubstituted product in 78% yield with moderate diastereoselectivity (up to 3:1).[21]

Table 1. Comparison between the reactivity of different ethyl organometallic derivatives in the nucleophilic addition to coumarin **7a**.

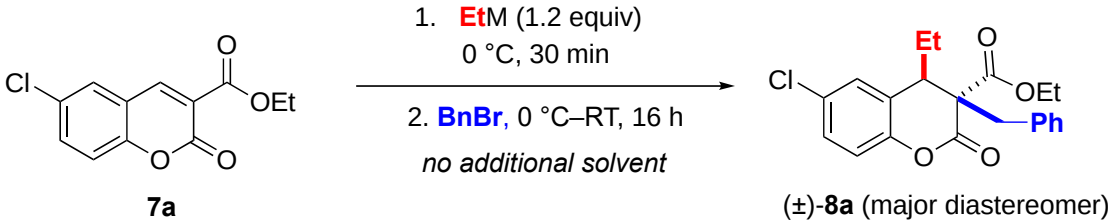

7a (±)-**8a** (major diastereomer)

Entry	EtM	Yield (%)[a]	dr[b]
1	EtLi	–[c]	–
2	Et_2Zn	–	–
3	Et_3ZnLi	71	90:10[d]
4	Et_4ZnLi_2	89	90:10[d]

[a] Yield refers to the major diastereomer isolated by column chromatography (see Experimental Section). [b] dr = diastereomeric ratio, determined by ^{1}H NMR analysis of the crude product. [c] Complex mixture of products. [d] Values refer to the following diastereomeric ratio: (3*R**,4*R**):(3*R**,4*S**).

With the aim to further extend the range of applications of homoleptic zincates, the direct nucleophilic addition of aliphatic and aromatic organozincates, followed by an interception with electrophiles, was in-depth investigated for the synthesis of stereodefined coumarin derivatives, following the same protocol reported in Entry 4 of Table 1 (Scheme 2). Furoyl and benzoyl chloride proved to be competent electrophilic partners as well, selectively delivering adducts (±)-**8b**,**c** in 55% and 60% yield, and with a dr up to 96:4 in favor of the (3*R**,4*S**)-diastereomer, further to the addition of Et_4ZnLi_2 and Me_4ZnLi_2 to **7a**, respectively. Similarly, the addition of other aliphatic zincate species, like Me_4ZnLi_2 and *i*-Pr_4ZnLi_2, to **7a** and the 6-iodo derivative **7b** proceeded smoothly, affording coumarins (±)-**8d**–**f** in 74–89% yield after quenching the mixture with BnBr, the dr being in between 89:11 and 96:4 on the side of the (3*R**,4*R**)-diastereomer. Conversely, the trapping reaction with aliphatic electrophiles, such as MeI and EtBr, has proven to be totally ineffective. We envisage that π-π stacking interactions between the coumarin ring and the (hetero)aryl group of the electrophile may be playing a key role in favoring a successful trapping reaction when using such aromatic electrophiles. On the other hand, (hetero)aromatic organozincate reagents, like Ph_4ZnLi_2 or 2-thienyl$_4$ZnLi$_2$, reacted with good reaction efficiency and high diastero- (dr 89:11) and chemoselectivity with **7a**, leading to (3*R**,4*R**)-configured coumarin derivatives (±)-**8g**,**h** in 81–88% yield, after the addition of BnBr (Scheme 2).

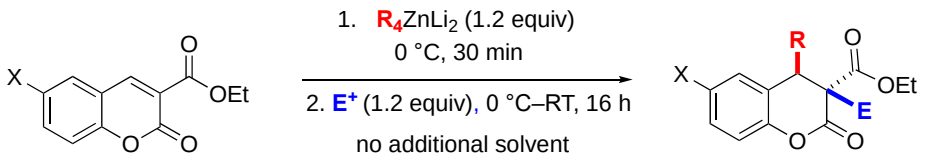

7a,**b**
(**7a**: X = Cl; **7b**: X = I)

(±)-**8** (major diastereomer)

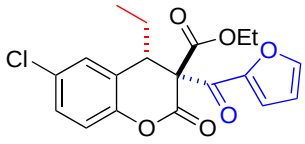

(±)-**8b**: 60%
dr: 96:4 [(3*R**,4*S**):(3*R**,4*R**)]

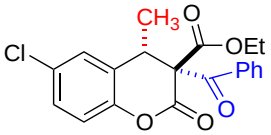

(±)-**8c**: 55%
dr: 90:10 [(3*R**,4*S**):(3*R**,4*R**)]

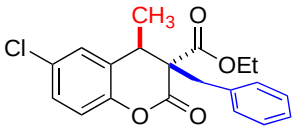

(±)-**8d**: 85%
dr: 90:10 [(3*R**,4*R**):(3*R**,4*S**)]

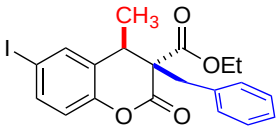

(±)-**8e**: 74%
dr: 96:4 [(3*R**,4*R**):(3*R**,4*S**)]

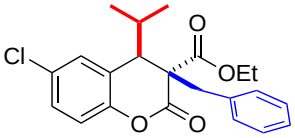

(±)-**8f**: 89%
dr: 89:11 [(3*R**,4*R**):(3*R**,4*S**)]

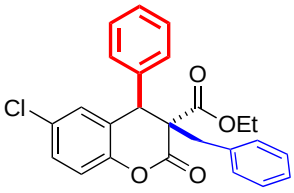

(±)-**8g**: 81%
dr: 89:11 [(3*R**,4*R**):(3*R**,4*S**)]

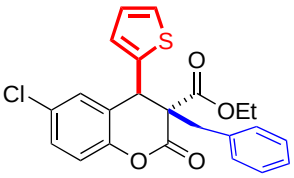

(±)-**8h**: 88%
dr: 89:11 [(3*R**,4*R**):(3*R**,4*S**)]

Scheme 2. Addition of R_4ZnLi_2 to coumarins **7a,b**, and sequential quenching with electrophiles, to give adducts (±)-**8**. Diastereomeric ratio (dr) determined by ^{1}H NMR analysis of the crude reaction mixture. Yield refers to the major diastereomer isolated by column chromatography.

The spatial arrangement of the substituents at the 3- and 4-positions on the lactone ring of compound (±)-**8a** was secured by combining 2D ^{1}H-^{1}H NOESY (Nuclear Overhauser Effect Spectroscopy) experiments with DFT calculations performed on both the diastereomers. The software used was ORCA 4.2.0. The geometry optimization was carried out at the DFT level by using the B3LYP functional and the 6-31G(d) basis set. For each optimized molecule, the vibrational frequencies were measured. They were all positive, thereby confirming that the structures were minima on the potential energy surface, and not transition states. All calculations were carried out in vacuum (for details, see Supporting Information).

From the ^{1}H-^{1}H NOESY spectrum of the major diastereomer of compound (±)-**8a**, the cross-peaks found between one of the two diastereotopic protons of the benzylic C*H*$_2$ at 3.12 ppm and the deshielded proton of the C*H*$_2$ of the ethyl group at 2 ppm are consistent with a close proximity relationship between these sets of protons, and thus with a relative (*R**,*R**) configuration (Figure 1). These findings are supported by DFT calculations carried out on both the two (*R**,*R**) and (*R**,*S**) diastereomers. As can be seen from Figure 2, the spatial arrangement of the (*R**,*R**)-diastereomer explains the diagnostic cross peak seen in the NOESY spectrum, and the reason for which only one of the two diastereotopic protons of the benzylic C*H*$_2$ (H_a) group and that of the deshielded proton of the C*H*$_2$ (H_c) of the ethyl group gave rise to a cross peak in the 2D H-H correlation spectrum. The distance between H_a and H_c was 2.2 Å, whereas the one between the H_b and H_d was 4.3 Å, which is too long to favor the transfer of nuclear spin polarization. As for the (*R**,*S**)-diastereomer, the distance either between H_a and H_c (4.5 Å) or between H_b and H_d (4.9 Å) was too long to result in a cross-peak (Figure 2). Thus, the joint combination of 2D NOESY and DFT calculations allowed us to assign the configuration to the major diastereomer, with the nucleophile and the electrophile being on the same side of the lactone ring. Such a conclusion could also be extended to the other coumarin derivatives (Scheme 2)

exhibiting similar NOESY spectra. For example, in the case of the diastereomer (±)-**8d**, the cross peak seen in the 2D NOESY spectrum between the protons of the methyl group at 1.47 ppm and that of the shielded proton of the benzylic methylene group at 3.32 ppm suggests a similar (*R**,*R**) spatial arrangement (Figure 1).

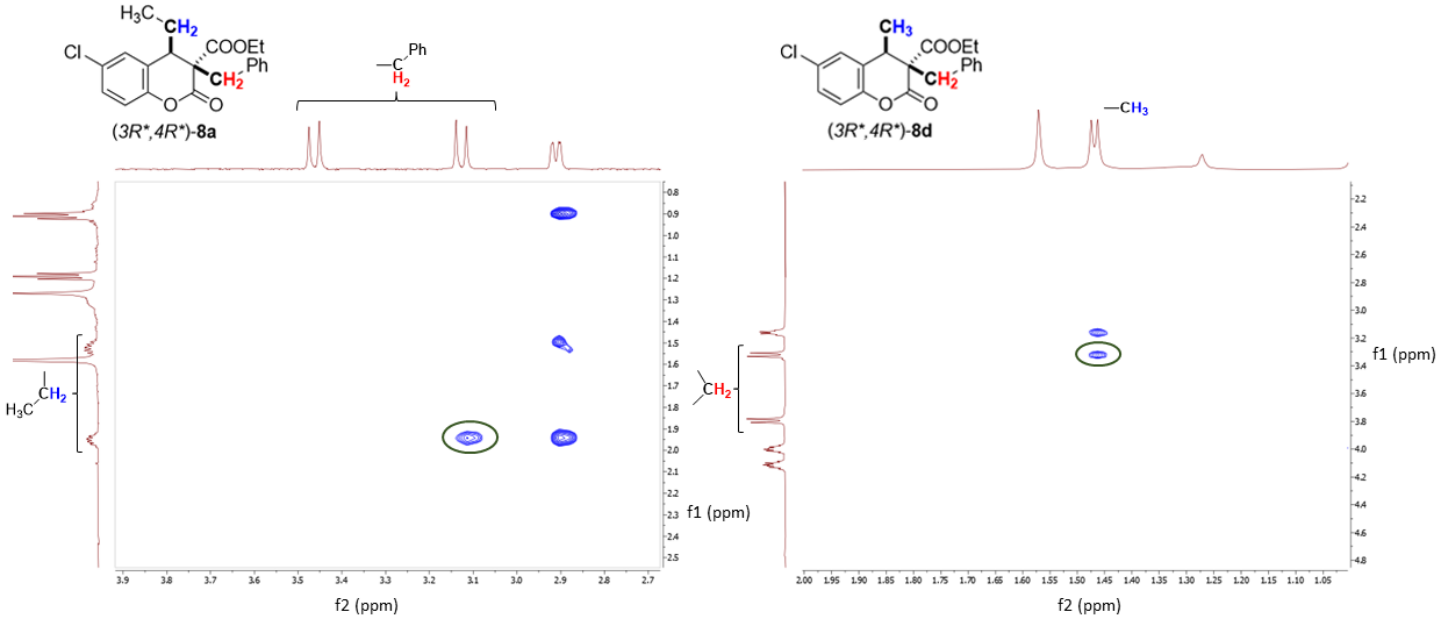

Figure 1. ^{1}H-^{1}H NOESY of diastereomers (3*R**,4*R**)-**8a** and (3*R**,4*R**)-**8d** in $CDCl_3$, with diagnostic NOE correlations circled in green.

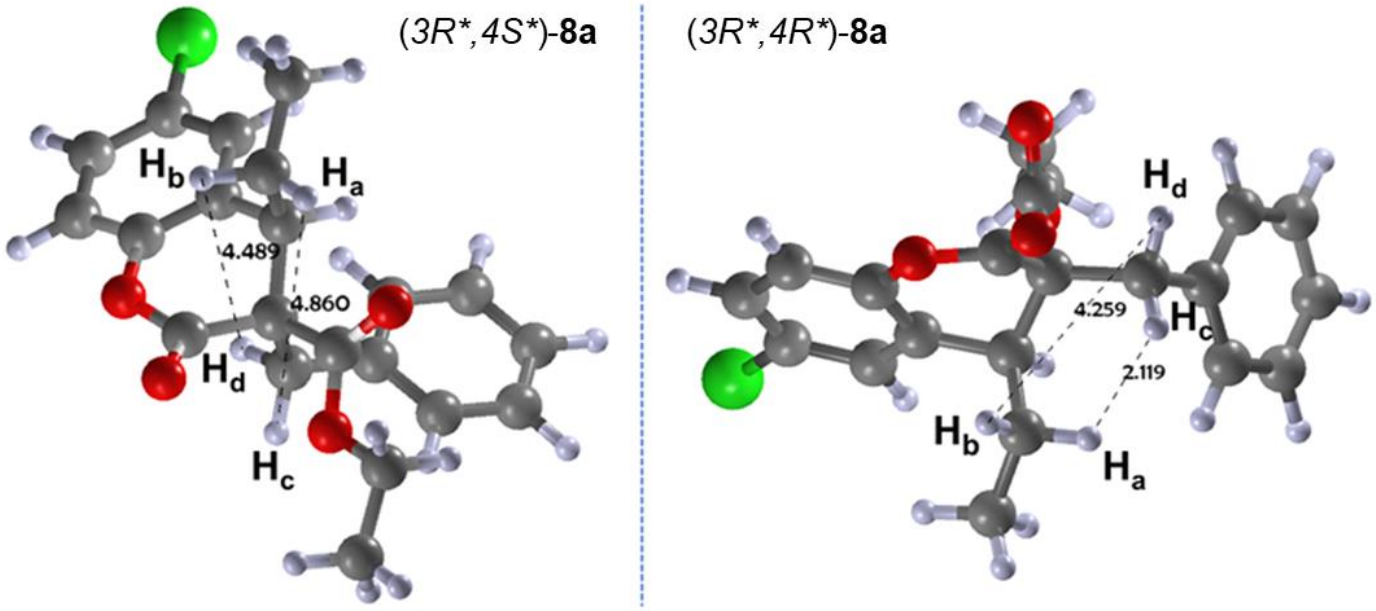

Figure 2. The spatial arrangement corresponding to the minimum of energy found by means of DFT calculations for (3*R**,4*S**)-**8a** (left) and (3*R**,4*R**)-**8a** (right).

DFT calculations suggest that the two possible spatial arrangements of the two diastereomers of (±)-**8a** have a comparable stability, that related to the (*R**,*R**) isomer being only +1.59 kcal/mol higher than that of the (*R**,*S**) isomer (Figure 3). Thus, the reaction might be under kinetic control, that is with the product ratio

being determined by the rate at which the two diastereomers form. Further studies are, however, necessary to shed light on the mechanistic aspects of such processes.

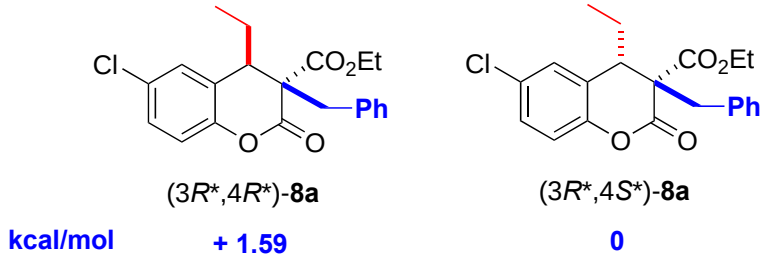

Figure 3. Relative energy values associated to the two possible diastereomers of adduct (±)-**8a**.

Conclusions

We have shown that the conjugate addition to the unsaturated lactone ring of coumarins can be conveniently carried out using high-order zincate species. Under mild (0 °C) and neat conditions, the addition of both aliphatic and aromatic organozincates, followed by the trapping reaction with external electrophiles, proceeds smoothly and with high chemoselectivity (without any competitive addition to ester groups or exchange reactions with halogen atoms), thereby delivering the desired adducts with high diastereoselectivity (up to 96:4) and in a very good yield (up to 89%). The stereochemistry of the major trisubstituted diastereomer was secured by 2D NOESY studies, supported by DFT calculations. This methodology could have a non-negligible impact in the field of heterocycle functionalization, especially considering the unique nucleophilicity and the exceptional functional group tolerance exhibited by alkali-metal zincate complexes in promoting selective and challenging organic transformations, which cannot be replicated by their monometallic counterparts.

Experimental Section

General. ^{1}H NMR and ^{13}C NMR spectra were recorded on a Bruker 600 MHz spectrometer and chemical shifts are reported in parts per million (δ). FT-IR spectra were recorded on a Perkin-Elmer 681 spectrometer. GC analyses were performed on a HP 6890 model, Series II by using a HP1 column (methyl siloxane; 30 m x 0.32 mm x 0.25 µm film thickness). Analytical thin-layer chromatography (TLC) was carried out on pre-coated 0.25 mm thick plates of Kieselgel 60 F_{254}; visualization was accomplished by UV light (254 nm) or by spraying a solution of $KMnO_4$ and heating to 473 K until yellow spots appeared. The solution of $KMnO_4$ was prepared by dissolving 1.5 g of $KMnO_4$, 10 g of K_2CO_3, and 1.25 mL of 10 % (w/v) solution of NaOH in 200 mL of water. Chromatography was run by using silica gel 60 with a particle size distribution 40–63 µm and 230-400 ASTM. GC-MS analyses were performed on HP 5995C model. High-resolution mass spectrometry (HRMS) analyses were performed using a Bruker microTOF QII mass spectrometer equipped with an electrospray ion source (ESI). Coumarin derivatives **7a** and **7b** were synthesized according to literature procedures.[22] The following solutions of organozinc and organolithium reagents were furnished by SigmaAldrich (Sigma-Aldrich, St. Louis, MO, USA), and were used with the following concentration: Et_2Zn 1.0 M in hexanes, EtLi 0.5 M in cyclohexane/benzene, MeLi 1.6 M in diethyl ether, Me_2Zn 2 M in toluene, *i*-PrLi 0.7 M in pentane, 2-thienylLi 1.0 M in THF/hexane and PhLi 1.9 M in dibutyl ether. Full characterization data, including copies of ^{1}H and ^{13}C

NMR spectra, have been reported for the synthesized compounds (±)-**8a**–**h**. The following abbreviations have been used to explain the multiplicities: s = singlet, d = doublet, dd = double doublet, t = triplet, q = quartet, m = multiplet.

Synthesis of Tetraorganozincate Species. Et_4ZnLi_2 was prepared through a co-complexation process: Et_2Zn (1 mL of a 1 M solution in hexane, 1 mmol) was added dropwise to a EtLi solution (4 mL of a 0.5 M solution in cyclohexane, 2 mmol). The resultant mixture was stirred for 1.5 h. Ph_4ZnLi_2 was prepared according to the literature.[23] *i*-Pr_4ZnLi_2 and 2-thienyl$_4ZnLi_2$ were prepared starting from the corresponding organolithium reagent (4 mmol, *i*-PrLi 0.7 M in pentane, 2-thienylLi 1.0 M in THF/hexane), through salt metathesis with anhydrous $ZnCl_2$ (1 mmol) according to literature procedures.[24]

Preparation of *i*-Pr_4ZnLi_2: *i*-PrLi (0.7 M in pentane, 4.0 mmol) was added to a stirred and cooled (0 °C) solution of $ZnCl_2$ (136 mg, 1.0 mmol) in dry Et_2O (5 mL). The mixture was stirred for 30 min at 0 °C prior to use.

Preparation of 2-thienyl$_4ZnLi_2$: 2-thienylLi (1.0 M in THF/hexane, 4.0 mmol) was added to a stirred and cooled (0 °C) solution of $ZnCl_2$ (136 mg, 1.0 mmol) in dry Et_2O (5 mL). The mixture was stirred for 30 min at 0 °C prior to use.

Nucleophilic Addition of Organozincates to Coumarin Derivatives: General Procedure. In a 25 ml round-bottom-flask charged with 0.5 mmol of substrate **7a** (or **7b**), the organozincate species, freshly prepared and handled under argon using conventional Schlenk techniques, was added (1.2 equiv) at 0 °C and under an argon atmosphere. Then, the resulting mixture was stirred for 30 min before being quenched with 1.2 equiv of electrophile. The mixture was left to stir overnight at room temperature before being extracted with EtOAc (3 x 15 ml). The resulting organic layers were collected, washed with brine, and the volatiles were removed under reduced pressure. The crude was purified by column chromatography on silica gel (hexane:EtOAc 15:1) to afford adduct (±)-**8**.

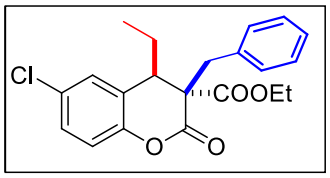

(3*R,4*R**)-Ethyl 3-benzyl-6-chloro-4-ethyl-3,4-dihydro-2-oxochroman-3-carboxylate (8a).** White solid, yield 89%. ^{1}H NMR (600 MHz, $CDCl_3$). 7.22-7.28 (m, 4H), 7.16 (d, *J* 1.8 Hz, 1H), 7.06-7.07 (m, 2H), 7.01 (d, *J* 8.6 Hz, 1H), 4.13-4.23 (m, 2H), 3.45 (d, *J* 14.1 Hz, 1H), 3.11 (d, *J* 14.1 Hz, 1H), 2.89 (dd, *J* 2.4 Hz, 4.8 Hz, 1H), 1.97-1.91 (m, 1H), 1.47-1.54 (m, 1H), 1.17 (t, *J* 7.1 Hz, 3H), 0.89 (t, *J* 7.2 Hz, 3H). ^{13}C NMR (150 MHz, $CDCl_3$). 168.4, 165.0, 149.0, 134.4, 130.1, 129.6, 128.6, 128.5, 128.2, 127.6, 126.5, 117.8, 61.9, 58.2, 44.2, 39.3, 29.7, 23.9, 13.9. GC-MS (70 eV) : *m/z* (%) 372 (M^+, 3), 326 (7), 299 (6), 281 (6), 235 (35), 168 (26), 91 (100). FT-IR (film, cm^{-1}). 3065, 3032, 2963, 2927, 2875, 2854, 1783, 1738, 1481, 1239, 1215, 1183, 1140, 1088, 1076, 1032. HRMS (ESI) *m/z* calcd for $[C_{21}H_{21}ClO_4+H]^+$: 373.1201; found: 373.1203; $[C_{21}H_{21}ClO_4+Na]^+$ calcd: 395.1021; found: 395.1023.

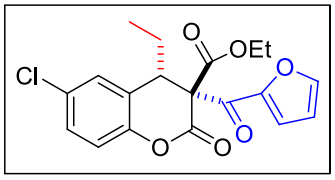

(3*R,4*S**)-Ethyl 6-chloro-4-ethyl-3-(furan-2-carbonyl)-2-oxochroman-3-carboxylate (8b).** White solid, yield 60%. ^{1}H NMR (600 MHz, $CDCl_3$). 7.60 (s, 1H), 7.28-7.27 (m, 1H), 7.22 (dd, *J* 8.6 Hz, 2.0 Hz, 1H), 7.05 (d, *J* 2.0 Hz, 1H), 7.00 (d, *J* 8.6 Hz, 1H), 6.55 (dd, *J* 3.6 Hz, 1.8 Hz, 1H), 4.26-4.20 (m, 2H), 3.77 (dd, *J* 10.4 Hz, 2.7 Hz, 1H), 1.31-1.23 (m, 2H), 1.13 (t, *J* 7.1 Hz, 3H), 0.98 (t, *J* 7.4 Hz, 3H). ^{13}C NMR (150 MHz, $CDCl_3$). 178.2, 164.9, 162.7, 150.2, 149.1, 147.0, 129.8, 129.0, 127.7, 126.5, 120.1, 118.2, 112.9, 62.6, 43.3, 29.7, 23.4, 13.7, 11.9. GC-MS (70 eV) : *m/z* (%) 281 (32), 235 (96), 95 (100). FT-IR (neat, cm^{-1}). 3198, 2922, 1779, 1748, 1673, 1566, 1463, 1388, 1233, 1154, 1088, 1035, 767. HRMS (ESI) *m/z* calcd for $[C_{19}H_{17}ClO_6+H]^+$: 377.0792, found: 377.0789; $[C_{19}H_{17}ClO_6+Na]^+$ calcd: 399.0606, found: 399.0610.

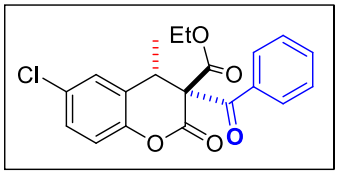

(3*R,4*S**)-Ethyl 3-benzoyl-6-chloro-4-methyl-2-oxochroman-3-carboxylate (8c).** White solid, yield 55%. ^{1}H NMR (600 MHz, $CDCl_3$). 7.73-7.71 (m, 2H), 7.56-7.54 (m, 1H), 7.43-7.40 (m, 2H), 7.24-7.22 (m, 1H), 7.09 (s, 1H), 6.98-6.97 (m, 1H), 4.19-

4.07 (m, 2H), 4.04 (q, *J* 6.6 MHz, 1H), 1.51 (d, *J* 7.2 Hz, 3H), 1.04 (t, *J* 7.2 Hz, 3H). ^{13}C NMR (150 MHz, $CDCl_3$). 191.5, 165.4, 163.8, 148.9, 135.8, 133.3, 129.7, 128.7, 128.5$_2$, 128.5$_0$, 127.8, 127.1,117.8, 62.7, 53.1, 36.8, 15.2, 13.6. GC-MS (70 eV) : *m/z* (%) 299 (1), 267 (21), 105 (100), 77(35), 51 (5). FT-IR (film, cm^{-1}). 3064, 2919, 2850, 1778, 1738, 1682, 1599, 1481, 1410, 1230, 1090, 1026, 890, 822. HRMS (ESI) *m/z* calcd for $[C_{20}H_{17}ClO_5+H]^+$: 373.0837, found: 373.0833; calcd for $[C_{20}H_{17}ClO_5+Na]^+$: 395.0657, found: 395.0657.

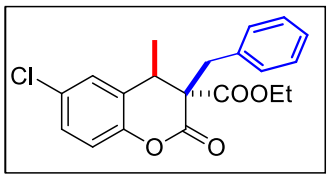

(3*R,4*R**)-Ethyl 3-benzyl-6-chloro-4-methyl-2-oxochroman-3-carboxylate (8d).** White solid, yield 85%.^{1}H NMR (600 MHz, $CDCl_3$). 7.30-7.23 (m, 6H), 7.17 (s, 1H), 6.98 (d, *J* 8.4 Hz, 1H), 4.14-4.09 (m, 1H), 4.02-3.97 (m, 1H), 3.79 (d, *J* 14.4 Hz, 1H), 3.32 (d, *J* 14.4 Hz, 1H), 3.16, (q, *J* 6.6 Hz, 1H), 1.46 (d, *J* 6.9 Hz, 3H), 0.99 (t, *J* 7.1 Hz, 3H). ^{13}C NMR (150 MHz, $CDCl_3$). 167.8, 166.5, 149.2, 135.0, 130.4, 129.9, 128.6, 128.3, 127.8, 127.4, 126.2, 117.4, 62.0, 58.1, 37.0, 33.9, 13.7, 13.6. GC-MS (70 eV). *m/z* (%) 358 (M$^+$, 13), 312 (20), 267 (38), 284 (14), 221 (100), 203 (19), 154 (23), 91 (94). FT-IR (film, cm^{-1}). 3064, 3013, 2928, 2852, 1747, 1484, 1455, 1352, 1217, 1083, 875, 820, 704. HRMS (ESI) *m/z* calcd for $[C_{20}H_{19}ClO_4+H]^+$: 359.1045, found: 359.1050; $[C_{20}H_{19}ClO_4+Na]^+$ calcd: 381.0864, found: 381.0871.

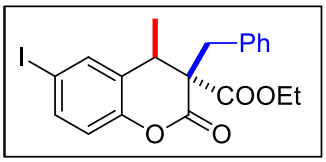

(3*R,4*R**)-Ethyl 3-benzyl-6-iodo-4-methyl-2-oxochroman-3 carboxylate (8e).** White solid, yield 74%. ^{1}H NMR (600 MHz, $CDCl_3$). 7.56 (d, *J* 8.4 Hz, 1H), 7.47 (s, 1H), 7.33-7.27 (m, 5H), 6.78 (d, *J* 8.4 Hz, 1H), 4.13-4.08 (m, 1H), 4.1-3.96 (m, 1H), 3.75 (d, *J* 14.4 Hz, 1H), 3.29 (d, *J* 14.4, 1H), 3.14 (q, *J* 6.6 Hz, 1H), 1.44 (d, *J* 7.2 Hz, 3H), 0.97 (t, *J* 6.6 Hz, 3H). ^{13}C NMR (150 MHz, $CDCl_3$). 167.8, 166.3, 150.4, 137.3, 135.0, 134.9, 130.4, 128.6, 128.5, 127.9, 127.4, 118.1, 62.0, 58.1, 37.1, 33.8, 29.4, 13.7. GC-MS (70 eV). *m/z* (%) 450 (M$^+$, 8), 359 (21), 313 (55), 246 (27), 203 (14), 91 (100), 65 (12). FT-IR (film, cm^{-1}). 2091, 2922, 2852, 1769, 1738, 1470, 1397, 1261, 1236, 1087, 801, 702. HRMS (ESI) calcd for $[C_{20}H_{19}IO_4+H]^+$: 451.0401, found: 451.0410; calcd for $[C_{20}H_{19}IO_4+Na]^+$: 473.0220, found: 473.0219.

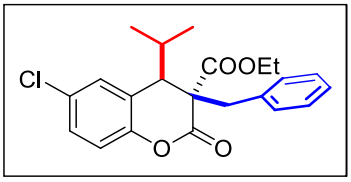

(3*R,4*R**)-Ethyl 3-benzyl-6-chloro-4-isopropyl-2-oxochroman-3-carboxylate (8f).** Colorless oil, yield 89%. ^{1}H NMR (600 MHz, $CDCl_3$) δ 7.29 (dd, *J* 8.6 Hz, 2.2 Hz, 1H), 7.20-7.19 (m, 3H), 7.13 (d, *J* 2.1 Hz, 1H), 7.02 (d, *J* 8.6 Hz, 1H), 7.98-7.97 (m, 2H), 4.35-4.27 (m, 2H), 3.39 (d, *J* 14.0 Hz, 1H), 3.08 (d, *J* 2.8 Hz, 1H), 2.86 (d, *J* 14.0 Hz, 1H), 2.01-1.96 (m, 1H), 1.33 (t, *J* 7.1 Hz, 3H), 0.98 (d, *J* 6.8 Hz, 3H), 0.72 (d, *J* 6.7 Hz, 3H). ^{13}C NMR (150 MHz, $CDCl_3$). 168.7, 163.9, 149.5, 134.2, 130.1, 129.8, 129.1, 129.0, 128.2, 127.5, 122.2, 117.6, 61.8, 57.5, 52.0, 41.8, 30.8, 22.2, 16.0, 14.0. GC/MS (70 eV) *m/z* (%). 386 (M$^+$, 5), 269 (12), 253 (25), 207 (45), 182 (96), 91 (100). FT-IR (film, cm^{-1}). 3064, 3031, 2964, 2934, 2877, 1790, 1727, 1482, 1455, 1417, 1368, 1390, 1368, 1274, 1243, 1137, 1077, 1038, 1006, 819, 699. HRMS (ESI). *m/z* calcd for $[C_{22}H_{23}ClO_4+Na]^+$: 409.1177, found 409.1188.

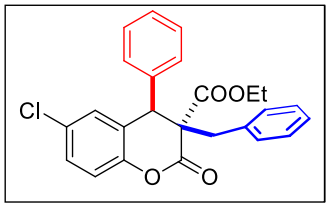

(3*R,4*R**)-Ethyl 3-benzyl-6-chloro-2-oxo-4-phenylchroman-3-carboxylate (8g).** White solid, yield 81%. ^{1}H NMR (600 MHz, $CDCl_3$) δ 7.29-7.22 (m, 7H), 7.11-7.04 (m, 5H), 6.98 (d, *J* 1.8 Hz, 1H), 4.30 (s, 1H), 3.93-3.88 (m, 1H), 3.77-3.72 (m, 1H), 3.69 (d, *J* 14.4 Hz, 1H), 3.08 (d, *J* 14.4 Hz, 1H), 0.88 (t, *J* 7.2 Hz, 3H). ^{13}C NMR (150 MHz, $CDCl_3$) δ 168.3, 164.1, 148.8, 137.8, 134.5, 130.2, 130.0, 128.9, 128.6, 128.4, 127.6, 126.0, 118.0, 61.9, 59.8, 40.8, 31.6, 13.3. GC-MS (70 eV) *m/z* (%) 420 (M$^+$, 4), 329 (20), 283 (58), 215 (100), 203 (72), 91 (59). FT-IR (film, cm^{-1}). 3031, 2919, 2850, 1780, 1726, 1455, 1481, 1215, 1247, 1139, 1076, 1029, 819, 698; HRMS (ESI) *m/z* calcd for $[C_{25}H_{21}ClO_4+H]^+$: 421.1201; found: 421.1205; *m/z* calcd for $[C_{25}H_{21}ClO_4+Na]^+$: 443.1021; found: 443.1024.

(3*R,4*R**)-Ethyl 3-benzyl-6-chloro-2-oxo-4-(thiophen-2-yl)chroman-3-carboxylate (8h).** Colorless oil, yield 88%. ^{1}H NMR (600 MHz, $CDCl_3$) δ 7.30 (d, *J* 5.2 Hz, 1H), 7.25-7.23 (m, 4H), 7.15 (dd, *J* 7.4 Hz, 1.6 Hz, 2H), 7.03 (d, *J* 8.6 Hz, 1H), 6.99 (dd, *J* 5.1 Hz, 3.6 Hz, 1H), 6.89 (d, *J* 2.3 Hz, 1H), 6.85 (d, *J* 3.5 Hz, 1H), 4.86 (s, 1H), 4.07-3.97 (m, 2H), 3.71 (d, *J* 14.3 Hz, 1H), 3.12 (d, *J* 14.3 Hz, 1H), 0.99 (t, *J* 7.2 Hz, 3H); ^{13}C NMR (150 MHz, $CDCl_3$). 167.9, 164.6, 148.5, 138.3, 134.5, 130.5, 130.3, 130.0, 128.9, 128.5, 128.3, 128.0, 127.6, 127.0, 126.4, 117.7, 62.3, 59.7, 44.0, 39.2, 13.4; GC/MS (70 eV) *m/z* (%). 426 (M^+, 4), 335 (25), 289 (57), 221 (100), 203 (26), 91 (44); FT-IR (film, cm^{-1}). 3031, 2850, 1767, 1736, 1780, 1454, 1411, 1367, 1246, 1212, 1125, 1077, 1030, 820, 700 cm^{-1}; HRMS (ESI). *m/z* calcd for $[C_{23}H_{19}ClO_4S+Na]^+$ 449.0585, found: 449.0594.

Acknowledgements

This work was financially supported by Ministero dell'Università e della Ricerca (MUR) through the PRIN project "Unlocking Sustainable Technologies Through Nature-Inspired Solvents" (NATUREChem) (grant number: 2017A5HXFC_002). The authors are indebted to Dr. Celeste Lanzellotto for her contribution to the experimental section.

Supplementary Material

Copies of ^{1}H and ^{13}C NMR spectra of compounds **8a**–**h** and details of DFT calculations are given in the Supplementary Material file associated with this manuscript.

References

1. Borys A. M.; Hevia E. *Trends Chem.* **2021**, *3*, 803. https://doi.org/10.1016/j.trechm.2021.07.006
2. Gil-Negrete J. M.; Hevia E. *Chem. Sci.* **2021**, *12*, 1982. https://doi.org/10.1039/D0SC05116K
3. Borys A. M.; Hevia E. *Angew. Chem. Int. Ed.* **2021**, *60*, 24659. https://doi.org/10.1002/anie.202110785
4. Uzelac M.; Mastropierro P.; De Tullio M.; Borilovi I.; Tarrés M.; Kennedy A. R.; Aromí G.; Hevia E. *Angew. Chem. Int. Ed.* **2021**, *60*, 3247. https://doi.org/10.1002/anie.202013153
5. Davin L.; Hernán-Gómez A.; McLaughlin C.; Kennedy A. R.; McLellan R.; Hevia E. *Dalton Trans.* **2019**, *48*, 8122. https://doi.org/10.1039/C9DT00923J
6. De Tullio, M.; Borys, A. M.; Hernán-Gómez, A.; Kennedy, A. R.; Hevia, E. *Chem. Catalysis* **2021**, *1*, 1308. https://doi.org/10.1016/j.checat.2021.09.016
7. Dell'Aera M.; Perna F. M.; Vitale P.; Altomare A.; Palmieri A.; Maddock L. C. H.; Bole L. J.; Kennedy A. R.; Hevia E.; Capriati V. *Chem. Eur. J.* **2020**, *26*, 8742. https://doi.org/10.1002/chem.202001521
8. Howell G. P. *Org. Process Res. Dev.* **2012**, *16*, 1258.

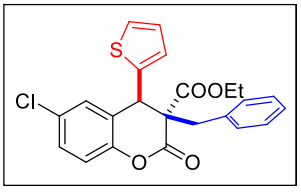

https://doi.org/10.1021/op200381w
9. Perlmutter P. *Conjugate Addition Reactions in Organic Synthesis*, Vol. 9, 1st Ed., Pergamon, Oxford, 1992, pp. 1–373.
10. Wu, Y.; Xu, J.; Liu, Y.; Zeng, Y.; Wu, G. *Front. Oncol.* **2020,** *10,* 592853. https://doi.org/10.3389/fonc.2020.592853
11. Qin, H.-L.; Zhang, Z.-W.; Ravindar, L.; Rakesh, K. P. *Eur. J. Med. Chem.* **2020,** *207,* 112832. https://doi.org/10.1016/j.ejmech.2020.112832
12. Kontogiorgis, C.; Detsi, A.; Hadjipavlou-Litina, D. *Expert Opin. Ther. Pat.* **2012,** *22,* 437–454. https://doi.org/10.1517/13543776.2012.678835
13. Delogu, G. L.; Matos, M. J. *Curr. Top. Med. Chem.* **2017,** *17,* 3173–3189. https://doi.org/10.2174/1568026618666171215094029
14. Squitti R.; Ghidoni R.; Siotto M.; Ventriglia M.; Benussi L.; Paterlini A.; Magri M.; Binetti G.; Cassetta E.; Caprara D.; Vernieri F.; Rossini P. M.; Pasqualetti P. *Ann. Neurol.* **2014**, *75*, 574. https://doi.org/10.1002/ana.24136
15. Kumar, N.; Udayabhanu; Alghamdi, A. A.; Mahadevan, K. M.; Nagaraju, G. *J. Mol. Struct.* **2021,** *1223,* 129208. https://doi.org/10.1016/j.molstruc.2020.129208
16. Sun, X.-y.; Liu, T.; Sun, J.; Wang, X.-j. *RSC Adv.* **2020**, *10,* 10826–10847. https://doi.org/10.1039/c9ra10290f
17. Abdel-Wahab B. F.; Mohamed H. A.; Farhat A. A. *Org. Commun*. **2014**, *7:1*, 1. https://doi.org/10.1002/ana.24136
18. Gustafsson B. *Finnish Chem. Lett.* **1975**, *2*, 49.
19. Gustafsson B.; Ostman K. *Acta Chem. Scand.* **1977**, *B31*, 425. https://doi.org/10.3891/acta.chem.scand.31b-0425
20. Bennabi S.; Narkunan K.; Rousset L.; Bouchu D.; Ciufolini M. A. *Tetrahedron Lett.* **2000**, *41*, 8873. https://doi.org/10.1016/S0040-4039(00)01506-9
21. Teichert J. F.; Feringa, B. L. *Chem. Commun.* **2011**, *47*, 2679. https://doi.org/10.1039/C0CC05160H
22. Bonsignore, L.; Cottiglia, F.; Maccioni, A. M.; Secci, D.; Lavagna, S. M. *J. Heterocycl. Chem.* **1995**, *32*, 573. https://doi.org/10.1002/jhet.5570320234
23. Hernan-Gomez, A.; Herd, E.; Uzelac, M.; Cadenbach, T.; Kennedy, A. R.; Borilovic, I.; Aromi, G.; Hevia, E. *Organometallics* **2015**, *34*, 2614. https://doi.org/10.1021/om501251q
24. Chau, N. T. T.; Meyer, M.; Komagawa, S.; Chevallier, F.; Fort, Y.; Uchiyama, M.; Mongin, F.; Gros, P. C. *Chem. Eur. J.* **2010**, *16*, 12425. https://doi.org/10.1002/chem.201001664